J. Condensed Matter Nucl. Sci. 15 (2015) 66–80

Research Article

Amplification and Restoration of Energy Gain Using Fractionated Magnetic Fields on ZrO_2–PdD Nanostructured Components

Mitchell Swartz*, Gayle Verner, Jeffrey Tolleson, Leslie Wright and Richard Goldbaum
JET Energy Inc., Wellesley Hills, MA 02481, USA

Peter Hagelstein
Massachusetts Institute of Technology, Cambridge, MA 02193, USA

Abstract

Lattice Assisted Nuclear Reactions (LANR) (CF) activated nanocomposite ZrO_2–PdNiD CF/LANR components are capable of significant energy gain over long periods of time with reproducibility and controllability. We report the response of such active components to steady and dynamic applied magnetic field intensities up to ∼1.5 T changing with a 0.1 ms rise time. Power gain was determined by the triple verified system of dT/P_{in}, HF/P_{in}, and calorimetry. Fractionated magnetic fields have a significant, unique amplification effect. Residual, late-appearing effects are complex. Importantly, at higher input electrical currents, high intensity fractionated magnetic fields demonstrate their own, new optimal operating point (OOP) manifold curve. This suggests that cold fusion (LANR) is the first stage, and may be mediated by other than phonons.
 ISSN 2227-3123

Keywords: Fractionated magnetic fields, Magnetic field intensities, ZrO_2PdD, Magnetic fields and CF/LANR

1. Introduction

1.1. Lattice Assisted Nuclear Reactions (LANR)

Clean, high efficiency energy production is critically important today, and in the foreseeable future, whatever the source may be. Lattice assisted nuclear reactions [LANR] enable deuterium fusion under difficult-to-achieve conditions in very highly hydrided Group VIII metals [1–23] in both aqueous [1–14] and nanomaterial systems [19–23]. This paper reports a method of increasing the excess heat output from such preloaded nanomaterial systems [19–23] (Fig. 1).

In the case of LANR in Pd and in some Ni and Ti systems, the apparent "excess" energy is heat which comes from the fact that there can rarely occur, in a lattice under special conditions, the fusion of two heavy hydrogen nuclei to form a helium nucleus [6,15–18]. The product helium, ^{4}He, is created new and fresh, generated directly from

*E-mail: mica@theworld.com

 ISSN 2227-3123

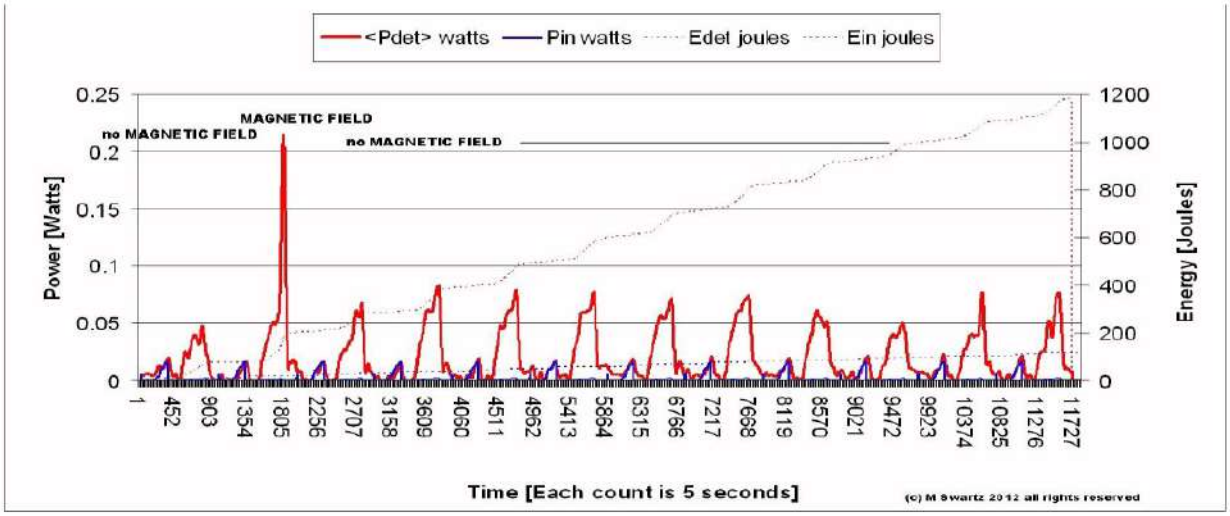

Figure 1. Impact of an applied Magnetic Field on a NANOR-type LANR component – Shown is the calorimetric response of a NANOR-type LANR component to the single application of a series of time-varying repeated high intensity H-field pulses (fractionated treatment between counts 1000 and 2000). The electrical input, and output, power and shown which reveal activity of the preloaded NANOR increasing during the fractionated treatment. Also shown are alternating thermal control, as well as background and calibration pulses. Power is read off of the left hand *y*-axis. The much lighter energy curves (dots) are read off of the right hand *y*-axis. Note the synchronous amplification of the NANOR power output induced by the magnetic field; this is not seen in the ohmic control. There is metachronous, longer-lasting, behavior which is no longer simply evanescent.

two, driven by more, deuterons physically located within the loaded palladium, nickel or one of their nanostructured materials. We speculate that the same, or similar, reactions occur here. Some of these materials have now been preloaded and made into high gain components, to create heat and other reactions with a very large energy density [19–23]. What is important is that the energy density of these CF/LANR components is quite considerable. Using the typical observed outputs, as described in this paper, the energy density and power density are orders of magnitude larger than conventional energy storage devices (Fig. 2).

Figure 2 shows the energy density and power density of these preloaded cold fusion, lattice assisted nuclear reaction components, in comparison to conventional, and recent, energy storage devices. These include the supercapacitor, nickel cadmium battery, lithium ion battery, lead acid battery, and fuel cell which are on the left-hand side of the graph.

As a result, LANR will play a critical role in all future technologies with potential revolutionary applications to all energy issues – robotics, transportation, electricity production, artificial internal organs, and space travel [1]. Most importantly, the product made by systems using CF/LANR is helium, which is environmentally safe and does not produce contamination.

1.2. Previous CF/LANR experiments

These reactions were first reported as aqueous systems called CMNS, LANR, LENR or cold fusion. Today, they involve palladium and/or nickel alloyed lattices or nanomaterials where the process occurs, generally irregularly at low efficiency. However, successful LANR requires engineering of multiple factors including loading, adequate confinement time (sometimes weeks), loading rate, and prehistory (with careful avoidance of contamination and materials and

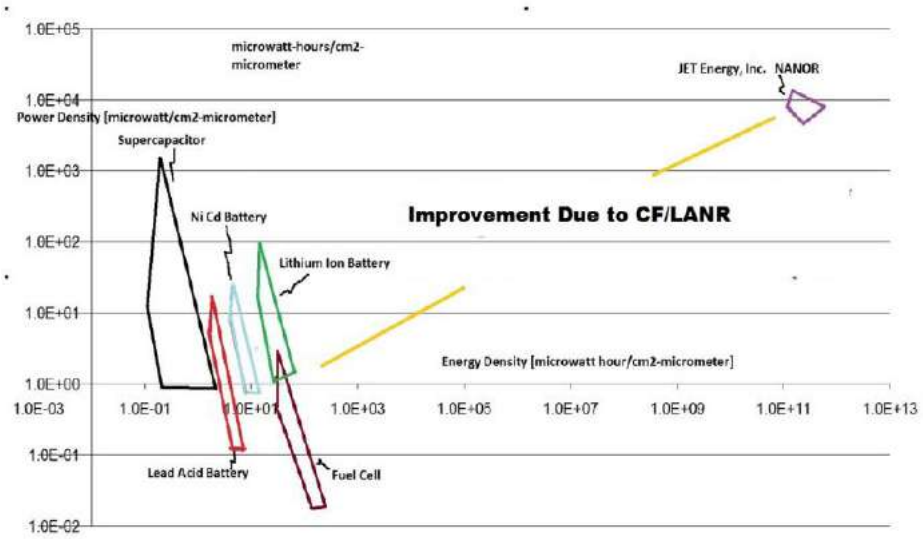

Figure 2. The energy density and power density of several energy production devices compared with the NANOR-type of CF/LANR component. Lattice Assisted Nuclear Reactions (LANR) have very high energy production densities .

operational protocols which quench performance). For example, we previously demonstrated this improvement of success in LANR aqueous systems, linked to high solution resistance (impedance) and shaped-metamaterial PHUSOR®-type LANR devices, with power gains more than 200–500%; and a wide range of power gains using codepositional high impedance devices DAP (Dual anode Phusor®-Type LANR device; Pd/D_2O, $Pd(OD)_2$/Pt–Au have reached ∼8000% compared to input power and to input power transferred to control dissipative devices (100%) [8–14].

However, our greatest findings so far, are that specifically, nanostructured materials, metamaterials, and their controlled operation improve success of both likelihood and power gain magnitude [15–18]. This paper presents the response of a new generation of preloaded LANR (CF) activated nanocomposite NANOR®$^{-\text{type}}$$ZrO_2$–PdNiD CF/LANR components, or devices, capable of significant energy gain [19–23] to dynamic applied magnetic field intensities.

1.3. Applied magnetic field intensities in CF/LANR

Magnetic and radiofrequency electromagnetic effects have been reported in aqueous CF/LANR systems [2–5,24]. In aqueous CF/LANR systems, steady magnetic fields have a small effect which include a decrease in cell electrical conductivity, if perpendicular to the direction of electrical current flow [24]. We report the first evidence of a fractionated magnetic field producing activation and rejuvenation of nanostructured CF/LANR material, reviving the output to higher levels than previously seen.

For this paper, we examined the impact of applied steady and dynamic (dH/dt) applied magnetic field intensities on NANOR-type CF/LANR devices during their significant energy gain. Controls included background, ohmic thermal controls, and long-term tests for time invariance and linearity, with and without the applied magnetic field intensities (∼1.5 T with 0.1 ms rise time × 1–5000 pulses).

One issue examined in particular was to determine that if there was an effect, the next question would be: is it similar to the near infrared (NT-NIR) emitted from active LANR materials and nanostructured materials, and to the

impact of optical and IR irradiation on LANR cathodes, where in both cases it was previously discovered and reported that such effects are maximized exactly when the CF/LANR devices are active at their peak optimal operating point [OOP; 12,14,15–18].

1.4. Active NANOR(R)-type LANR components

The two-terminal, NANOR®-type LANR devices are a new generation of active LANR (CF) preloaded, self-contained, reproducibly active, nanostructured nanocomposite ZrO_2–PdNiD CF/LANR devices capable of significant, reproducible excess heat from applied electric fields [19–23], and which have had portability enabling a range of investigations not previously possible. By self-contained, it is meant that the fuel is preloaded without the need for additional D sources, in liquid or gas. By portability, we refer to the fact that previously running a complete working CF/LANR system (aqueous high impedance PdD) required at least the equivalent of two desk sized volumes. In contrast, that requirement has now, with the preloaded NANOR-type CF/LANR component, been reduced to less than ∼one desktop surface equivalent. Thus, there is superior handling properties because of the fact that there are several types of additional equipment which are no longer required (to load before activation). This eliminates gas tanks, regulators, some types of power supplies and loading systems with their requisite temperature control, supplies of loading material, components holders, leads, electrical and gas connectors. They have all been made moot by the preloading of this component.

Their active CF/LANR core is ZrO_2–(PdNiD) and the like, loaded with additional D and H, yet dry and glued into an electrically conductive, sealed, configuration (Fig. 3a). The left figure shows two last-generation NANOR-type CF/LANR components revealing the core nanomaterial in a transparent way. The present NANOR has ZrO2–PdNiD nanostructured material at the core.

One such NANOR system was driven for more than a year with careful evaluation for energy gain under a variety of conditions, including during the January, 2012 IAP MIT Course on CF/LANR, and later during a long term low-power open demonstration at MIT which ran from Jan. 30, 2012 through mid May 2012 [20]. The NANOR®-type

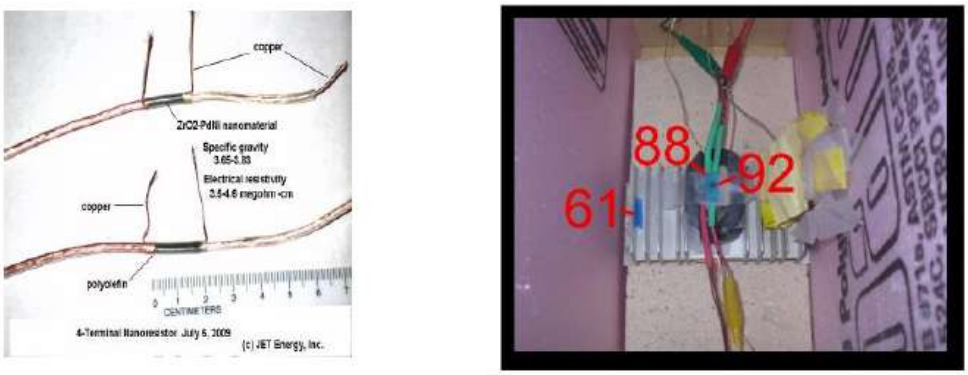

Figure 3. (a) The left figure shows two last-generation NANOR-type CF/LANR components revealing the core nanomaterial in a transparent way. The present NANOR has ZrO_2-PdNiD nanostructured material at the core. (b) The right hand side shows the physical arrangement used for exposure of a functioning Series VI NANOR and an ohmic control to the high intensity fractionated applied magnetic field. To show the arrangement and locations, the calorimeter was stripped of all thermal ballast, thermal conductive layers, electrical connectors, temperature sensors, probes, heat flow sensors, and insulating layers (both thermal and electrical) to reveal the physical arrangement of the CR-39 chips, the NANORő, the ohmic control, the housing and shielding .

preloaded LANR device openly demonstrated clearcut energy gain and features including its convenient size and its superior handling properties which arise because loading has been separated from activation. Over several weeks, time integration with calibration by the ohmic controls revealed that the NANOR®-type LANR device demonstrated more reproducible, controllable, energy gain (COP) which ranged generally from 5 to 16 (14.1 (∼1412%) in the steady state (∼hour) while the MIT IAP course was ongoing).

The NANOR® used for this work is a sixth generation CF/LANR device, smaller than 2 cm, with less than a gram of active material. However, this is actually a matter which is not *de minimus* because the LANR excess power density was more than 19,500 W/kg of nanostructured material. The later-designed preloaded NANOR®s can be fashioned into easily activated LANR (CF) Integrated Circuits which enable an entire new generation of ZrO_2–PdNiD preassembled IC electronic devices. The importance is that they enable LANR devices and their integrated systems to now be fabricated, transported, and then activated. They are the future of clean, efficient energy production.

1.5. Electronic properties of CF/LANR nanomaterials

Close up, in ZrO_2–PdNi-D LANR/CF nanostructured materials, the lattice of Pd is expanded by Zr, and less so, by the H and D. In addition, there are other major changes secondary to the oxidation of the Zr. We speculate that the nanomaterial, ZrO_2–(Pd_xNi_{1-x}), is a composite distribution of nanostructured ferromagnetic "islands" separated among a vast dielectric zirconia "ocean". We surmise that the dielectric zirconia embeds uncountable numbers of nanostructured metal ternary alloy islands of the material containing now NiPdD. The appearance is like a chocolate chip cookie on the nanoscale. The "chips" are composed of hydrided palladium nickel metallic alloy embedded in a zirconium oxide dielectric matrix ("cookie").

Electrically, the response of the CF nanostructured material is complex. The zirconia dielectric matrix is insulating at low voltage and it keeps the nanoscale metal islands electrically separated. It also prevents the aggregation of the islands. Each nanostructured island acts as a short circuit element during electrical discharge. These allow deuterons to form what is believed to be a hyperdense D-state in each island, where the deuterons are able to be sufficiently close together and "locked in".

In addition, CF/LANR nanomaterials are characterized by complicated polarization/transconduction phenomena including an "avalanche (transconduction electrical breakdown) effect" which has a critical role in excess heat generation [19–23]. We previously reported sudden changes of, and generally large, electrical impedances of such NANOR®-type devices containing nanostructured materials. Several were ∼3 mΩ when lower voltages were applied, but then as the voltage was increased to ∼24 V, the impedance suddenly decreased to very low values. It was shown theoretically that this sudden reduction can be attributed to an "avalanche effect" that is typical of the current–voltage behavior that occurs in Zener diodes. Keys to achieving success in CF/LANR include electrical engineering (continuum electromechanics and the Navier–Stokes equation to handle flow) as well as material science and metallurgy. Control of the breakdown states and quenching tendencies has been critical. Great difficulties have had to be surmounted including assembly of apomaterials of very high electrical resistivity (impedance), as high as 300 gΩ, creating several serious problems.

2. Experimental

2.1. Materials – active LANR nanostructured materials

We have surmounted many of these problems and previously reported the manufacture of NANOR®s and the production of excess heat using nanomaterial palladium, nickel, and newer alloyed compounds, such as ZrO_2PdNi. However, on the difficult side, to make preloaded nanocomposite LANR/CF materials into dry electronic circuit devices requires preparing active nanostructured materials from improved very pure materials, control and avoidance of low-threshold

breakdown of states and the quenching tendencies of nanostructured materials, and surmounting their extremely high electrical resistances and "avalanche (transconduction electrical breakdown) effect" [19–23].

For these NANOR-type LANR devices, it is believed that the fuel for the nanostructured material is contained within the core is palladium deuteride, itself within the zirconia nanostructured material. Nanostructured powders, such as Zr 67% Ni 29% Pd 4% (by weight before the oxidation step), absorb a very large number of deuterons for each and every nickel and palladium nuclei. There are reports of numbers in the order of 3.5, and perhaps higher. These include ZrO_2–PdNiD, ZrO_2–Pd, ZrO_2–NiD, and the like. The NANOR-type of LANR device is designed to contain the active ZrO_2/PdD nanostructured material in its core volume, or chamber. At JET Energy, Inc., the core that have been developed and used is ZrO_2–(PdNiD) with augmented processing including entrapping additional D and H using several proprietary processes and apparatus. The deuterons are tightly packed ("highly loaded"). The additional D yields apparent indicated loadings (ratio to Pd) of more than 130% D/Pd, but shallow traps are not ruled out. For simplicity, all of these nanostructured materials in the core, in their range of deuterations, will henceforth simply be referred to as ZrO_2–PdD.

This preloading system has achieved impressive results of excess heat over many months. Most importantly, the activation of the desired LANR reactions is, for the first time at room temperature, separated from the loading of the LANR substrate.

It is a long, expensive, arduous, effort to prepare these preloaded nanocomposite dry CF/LANR devices, whose development has required control of their breakdown states and quenching tendencies. The path to development has not been easy. There are important issues also involving particle size, electrical conductivity, and aggregation, that will be mentioned briefly, and some involve a large literature, beyond the scope of this publication. First, the size of nanostructured materials is key. The desired nanostructure islands of NiPdD have characteristic widths of 2–70 nm size, with the theoretical being less than the observed by imaging. The vibrations of nanostructured materials are believed to be very important for successful CF/LANR activity, and are reported to be maximized with softening of the material; and are important because they do couple the excited state of ^{4}He* to the ground state, and because they might also be of such amplitude that they can cause a sudden structural phase change to a lower free energy state.

Second, preparation of active nanostructured materials, able to undergo preloading, requires very pure materials. Contamination remains a major problem, with excess heat potentially devastatingly quenched. Contaminants can appear from both electrode and container degradation and leeching, from atmospheric contamination, especially after temperature cycling. Furthermore, the heavy water and D_2 are hygroscopic, therefore must be kept physically isolated from the air by sealing.

Third, potential toxicity must be considered. Nanostructured and nanocomposite materials have potential human and environmental health hazards. The large number of particles, and greater specific surface area, yield increased absorptive risk through the skin, lungs, and digestive tract. The preloaded nanostructured material is placed into the hermetically sealed enclosure which is specially designed to withstand pressure, minimize contamination, enable lock on of wires connecting to it. The enclosure is tightly fit with the electrodes. This is important because contamination is a potential problem, and because of the potential toxicity issue. In briefest summary, the production of the preloaded core material involves preparation, production, proprietary pretreatment, loading, post-loading treatment, activation, surmounting the extremely high electrical resistances, and then adding the final structural elements, including holder and electrodes. These are assembled to create the complete preloaded LANR nanomaterial package. When done properly, the result is a very useful and more reproducible nanostructured preloaded ZrO_2–PdD device which can be thereafter, remotely, easily activated, driven by an electrical circuit and controlled by an electrical driver. The component weighed about 80 times the weight of the core active material.

2.2. Methods – electrically driving the materials

The LANR preloaded, stabilized NANOR®s are driven by a high voltage circuit up to 3000 V rail voltage, which is the high voltage that can be delivered in any run to either the NANOR or the ohmic control. The duty cycle was split with half going to a control portion consisting of a carefully controlled electrical DC pulse into an ohmic resistor which was used to thermally calibrate the calorimeter. Input power is defined as $V \times I$. There is no thermoneutral correction in denominator. Therefore, the observed power is a lower limit. The instantaneous power gain [power amplification factor (non-dimensional)] is defined as P_{out}/P_{in}. The energy is calibrated by at least one electrical joule control [ohmic resistor] used frequently, and with time integration for additional validation. The excess energy, when present, is defined as ($P_{\text{output}} - P_{\text{input}}$) * time.

2.3. Methods – Thermometry and DAQ

Data acquisition is taken from voltage, current, temperatures at multiple sites of the solution, and outside of the cell, and even as a 4-terminal measurement of the NANOR®'s internal electrical conductivity. Data acquisition sampling is at data rates of 0.20–1 Hz, with 24+ bit resolution (e.g. Measurement Computing (MA) USB-2416, or a Omega OMB-DaqTemp or equivalent; voltage accuracy $0.015^{\pm 0.005}$ V, temperature accuracy $<0.6^{\circ}$C). All connections are isolated when possible, including where possible with Keithley electrometers, or their equivalent, for computer isolation. All leads are covered with dry, electrically insulating tubes, such as medical grade silicone, Teflon, and similar materials, used to electrically isolate wires. To minimize quantization noise, if necessary, 1 minute moving averages may be used for some signals. The noise power of the calorimeter is in the range of $\sim$1–30 mW. The noise power of the Keithley current sources is generally $\sim$10 nW.

2.4. Methods – verifiable calorimetry

The amount of output energy (and therefore, both power, and energy, gain) is determined from the heat released producing a temperature rise, which is then compared to the input energy. Observed signals are determined by parallel diagnostics including thermometry, focused heat flow measurement, and isoperibolic calorimetry, and then semiquantitively repeatedly calibrated by an ohmic (thermal) control located next to the NANOR®. The result is heat measurement of this preloaded NANOR®-type LANR three (3) ways ending in calorimetry, input-power-normalized ΔT (dT/P_{in}), and input power normalized heat (HF/P_{in}).

The output of the NANOR® is compared to the output of the precisely driven ohmic control (Fig. 4a). The instantaneous power gain is kinematically determined by the ratio of the input power normalized temperature increase to the input electrical power (P_{in}), called by the symbol '$\Delta T/P_{in}$' referring to the increase of temperature (ΔT) divided by the input electrical power. Also, the output of the NANOR® is independently derived by kinematically evaluating the heat flow, using the ratio of the input power normalized heat flow to the input electrical power (P_{in}), called by the symbol 'HF/P_{in}' referring to the heat flow (HF) divided by the input electrical power. The third method is examination by calorimetry, calibrated by the thermal ohmic control and thermal waveform reconstruction, and confirmed by long-term time integration. These three methods of verification are pooled to derive very useful information, including the energy produced ("excess energy") and sample activity ("characteristic or largest incremental power gain over an ohmic control").

2.5. Methods – applied magnetic field intensity

For this paper, we examined the response of NANOR®-type preloaded LANR devices containing active ZrO_2–PdD and ZrO_2–PdNiD nanostructured materials to steady state (continuous) magnetic fields, and then dynamic, rapidly

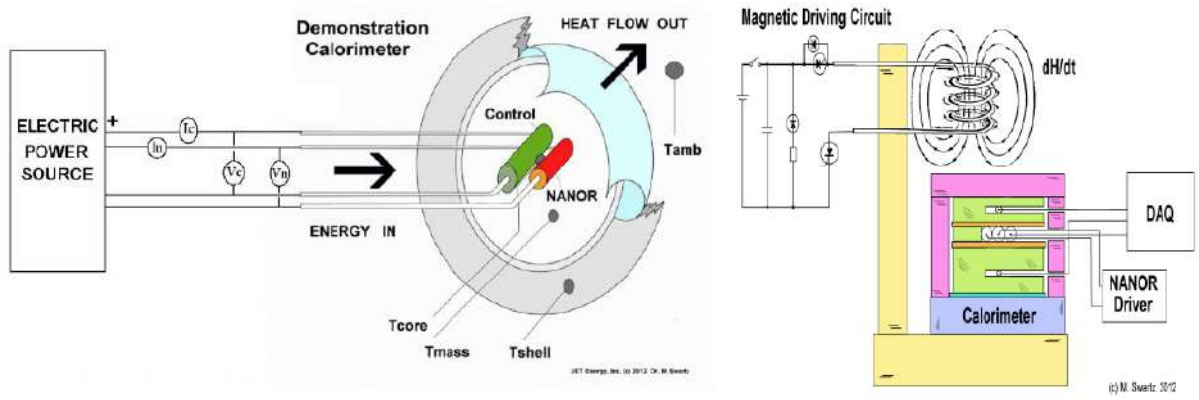

Figure 4. (*Left*) Schematic electric driver and calorimeter showing parallel diagnostics consisting of heat flow measurement and temperature, and the ohmic (thermal) control. (*Right*) Two terminal NANORő-type devices containing active ZrO_2–PdNiD nanostructured material at their core, with DAQ under the applied (off axis) dynamic magnetic field intensity. Next to it are the ohmic control, a temperature measurement device. The ballast with additional temperature measurements and calorimeter are shown only figuratively .

changing and then successively reapplied (fractionated) magnetic field (H-field) intensities. In the latter, the CF/LANR system ran while an H-field pulse sequence was delivered (dH/dt ∼1.5 T with 0.1 ms rise time × 1000–5000 pulses). The set-up is shown in Fig.3b and Fig 4b. Figure 3b shows the calorimeter stripped of said thermal materials and probes to reveal the physical arrangement of the CR-39 chips, the NANOR®, the ohmic control, the housing and shielding. The NANOR® and its active site are marked at #92. #88 labels the ohmic control. #61 labels the nearby control CR-39 chip, partially shielded by aluminum. The thermal materials *et alia* were replaced for the experiments. In Fig. 4b, the magnetic field lines continue into the housing and into and about the NANOR and the ohmic control. They are not shown in the diagram of Fig. 3b for convenience. The NANOR Explorer (the driver) is not shown. The fractionation refers to the sequence of multiple pulses, which in this case had rise times listed above.

Controls included background, ohmic thermal controls, tests for time invariance, with and without the applied magnetic field intensities. As controls, we ran simultaneous ohmic systems, and also used previous long term checks of the system and CF/LANR NANOR®-type component without fractionated (and static) H-fields, including with calibrations, and evaluations, along with the previous reports at ICCF-17. These reported on the importance of careful paradigms, intercalated controls, and demonstrated reasonable time invariance and linearity (except during the infrequent outgassing condition also reported, also reported where the excess power goes to zero).

Each pulse sequence was delivered at 1 Hz to the control and NANOR, but with the electrical current drive to the thermal ohmic control and then the NANOR®. This enabled determining the impact of the H-field upon the background, and upon the control, and upon the NANOR®. Times of these experimental cycles were longer compared to those discussed at ICCF-17 or used at the MIT IAP demonstration system because it was felt that long time constants might be involved (e.g. magnetization, possible additional energy transfer). A proprietary autonomous system was used to run the NANOR® continuously alternating with background and an ohmic thermal control. This was used to control the system which included a complementary, surrounding calorimeter. The proprietary microprocessor-controlled system semiquantitatively examines and drives the NANOR®, examining it for heat-production activity, linearity, time-invariance, and even the impact of additives and applied fields.

Power gain was determined by dT/P_{in}, HF/P_{in}, and calorimetry, but did not include the impact of the H for two reasons. First, it was transient, and not present in the vast amount of data. Second, it was also impinging upon the

controls which were monitored for the impact of the H-field upon it (ohmic resistor) at the same distance location, next to the NANOR®, and with electrical currents also going through it.

3. Results

3.1. DC magnetic fields

Static applied ("DC") magnetic fields have an small effect upon the active NANOR®-type nanomaterial CF/LANR systems, increasing power gain, especially at higher input electrical currents. Under that condition, and not seen in the controls, the applied static magnetic field intensities did produce a small to moderate increase gain (Fig. 5). They also produced some low intensity long-term (called 'metachronous') effects. These metachronous changes were reflected as a slight loss of near time-invariance. This effect was increased irregularity in the CF/LANR excess power output, post applied steady magnetic fields (and as discussed below, was also seen with the application of dynamic magnetic fields. As will be shown below, this is a minor effect compared to what was wrought by the applied high intensity fractionated magnetic fields, which will be shown to create both simultaneous and late (metachronous) major effect (*vide infra*).

3.2. d*H*/d*t* Magnetic fields – synchronous effects

In this case, it was discovered that high intensity, dynamic, repeatedly fractionated magnetic fields have a major, significant and unique synchronous amplification effect on the preloaded NANOR®-type LANR device under several

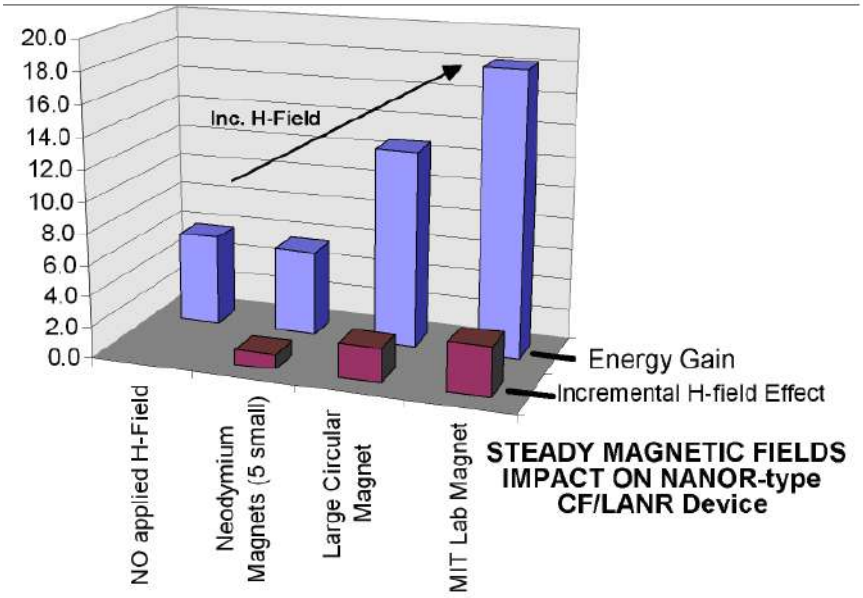

Figure 5. Impact of DC H-field Intensity on NANOR®-type LANR component – Energy gain and incremental H-field amplification for the LANR NANOR® Output as effect by an applied steady (DC) magnetic field intensity.

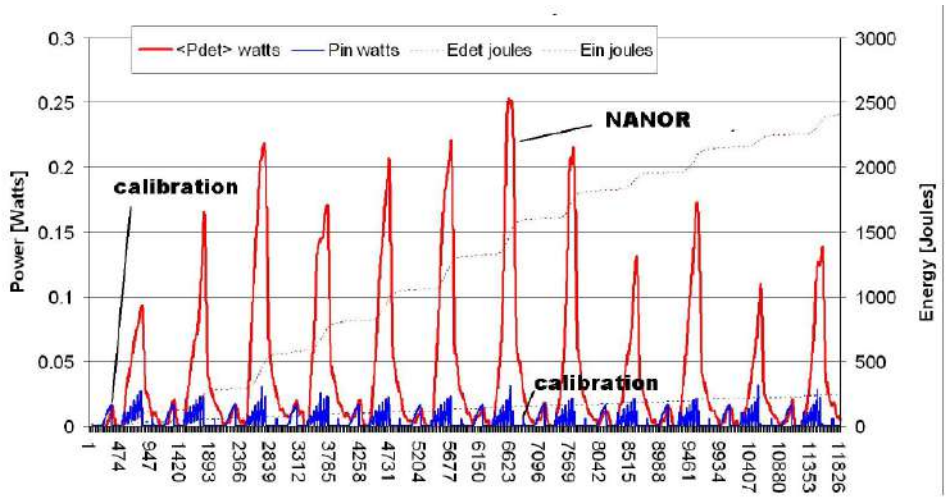

Figure 6. Input power and output heat flow normalized to input electrical power of a self-contained CF/LANR quantum electronic component at 124 V peak input voltage. There is also enhanced improvement of CF/LANR (which is synchronous), and there is improved of CF/LANR which is metachronous and longer-lasting.

conditions of operation. Synchronous effects are those caused by the applied high intensity fractionated magnetic field imposed upon the NANOR during the NANOR®s power gain during the run.

The magnetically treated preloaded NANOR®-type LANR devices had significant incremental power gain, and had – over a prolonged amount of time – higher efficiency excess heat production. This incremental gain was a significant improvement over all previous NANORs, and in fact, was an increase in power gain which is significant and far beyond that of CF/LANR alone.

For example, previously, the preloaded nanostructure devices [NANOR®s] had a significant energy gain, such as in the MIT 2012 demonstration unit (Energy gain $\sim 14\times$). By contrast, now, in this series of experiments involving investigating the possible impact of dH/dt, the CF/LANR NANOR® components demonstrated even higher gains. The incremental impact of the applied high intensity fractionated magnetic field treatments yielded a major synchronous effect on the power gain as determined by dT/P_{in}, HF/P_{in}, and calorimetry. The peak power gain was ranged from 22 to up to $\sim$80 times input electrical power or more beyond the control, as determined by calorimetry.

The input power provided to produce the H-field was not included, because consistent with this approximation it should be noted that there was no change in the output of the ohmic control, or with the background, and that the was no further H-field input beyond the first hour. Further evidence that the H-field has negligible input by energy is revealed by the negligible change in currents to the ohmic control and background (no electrical input) regions.

Most importantly, there was an increase over ordinary active cold fusion operation of these NANOR-type systems. The application of dH/dt created an increase of 4–10 times the peak power gain over "conventional" CF/LANR, "conventional" means the observed output of the same NANOR-type system before said application of repetitively fractionated magnetic field.

It is important to note that this effect was not observed in the controls through which currents are also applied during their share of the duty cycle. This effect was not observed for NANOR®s in place with no additional current driving them. This major level of impact only seen for the preloaded NANOR®-type LANR device when it was already putting out excess energy. This major level of impact was not observed for static magnetic fields.

3.3. Residual (metachronous) effects

Other effects were noted. Astonishingly, it has now been discovered that high intensity, dynamic, repeatedly fractionated, magnetic fields have an incremental major, significant and unique, complex, metachronous amplification effect on the preloaded NANOR®-type LANR device (cf. Figs. 6 and 1).

It is important to consider this *de novo* magnetic behavior. Perhaps this is expected for the nickel containing NANORs, but it is somewhat surprising for the palladium NANORs. Nickel is ferromagnetic and the induction of magnetization is to be expected. Not so normally for palladium.

However, under some conditions involving vacancies, the conversion of Pd from paramagentic to ferromagnetic behavior has been reported [25–28]. Palladium, like platinum, have potential as exchange-enhanced paramagnetic materials. When the Stoner criterion is satisfied, in response to external stimuli such as applied E-field, they exhibit unconventional magnetic responses – they become exchanged-enhanced ferromagnetic.

Palladium exhibits a strong Stoner enhancement. Pd has been reported, positioned between ultrathin ferromagnetic films, to become ferromagnetic [25]. With Pt, an electric gate voltage can induce an anomalous Hall effect (AHE) in the Pt thin film. The applied electric field can induce a magnetic moments as large as $\sim$10 μB in materials which can self interact, as described by the Langevin function [26]. Theoretically, this is supported by density-functional calculations [27]. The Fermi-level density of states drives the transition at the surface to an itinerant ferromagnetic state above a critical applied electric field intensity, E_c, and follows a square-root variation with electric field. This appears to be driven by vacancies in Pd (theoretically, up to 15% calculated using the SCR Korringa–Kohn–Rostoker coherent potential approximation method, which predicts a magnetic at $\sim$10% vacancies) [28]. We have recently begun to image the induced domains [29].

There has been long term metachronous impact wrought upon the treated CF/LANR NANORs, long after the treatment, heralded as increased power and energy gain as determined by dT/P_{in}, HF/P_{in}, and calorimetry. There was also an improvement of CF/LANR activity which was metachronous – and that means longer-lasting. Metachronous effects are those physical changes wrought by the applied high intensity fractionated magnetic field upon the function of the NANOR®s power and energy gain *after* the run. This is in addition to the enhanced improvement of CF/LANR operation by the dynamic magnetic treatment which is synchronous.

These wrought late-appearing, long lasting complex effects, including variable changes in activity, are significantly important. Operationally, the application of these high intensity fractionated magnetic fields had significant long term effects, which eliminate the previous near linearity of the output.

Instead there appear further time-complex findings, including the demonstration of increased irregularity and time variance of the energy gain, and what appear to have a component of cyclical changes in activity, rather than the simple exponential falloff seen previously extending over weeks [19–23].

This amplification of CF/LANR by dynamic magnetic fields and especially the significant, residual post-applied fractioned magnetic fields effects (which are complex and demonstrate variable, including cyclic, changes in activity) suggest a new CF/LANR material science/nuclear interaction.

3.4. New optimal operating point manifold

Now that both synchronous and metachronous effects have been discussed, it is important to shift to consider the incredible, newly discovered changes in optimal operating point (OOP) operation of the CF/LANR components. Previously, all cold fusion systems and the NANOR®s have always shown a single optimal operating point manifold for excess heat operation. That is no longer accurate after only a single treatment to a high intensity fractionated magnetic field. Instead, there now appear, uniquely, two OOP manifolds (Fig. 6).

Figure 7 shows the two OOP manifolds, as well as the ohmic control ("normal") response (defined here as '100%') and conventional CF/LANR operation ("cold fusion"), and the synchronous and metachronous impacts of a fraction-

ated magnetic field intensity. There is an amplified (phonon) OOP bigger than before, and an entirely new, *de novo* (magnon?) OOP. By this terminology, the authors mean an OOP enabling successful control of CF/LANR which is itself "catalyzed" by phonons (and magnons, respectively) in that de-excitation from the 24 MeV excited $^{4}*$ can only occur by an adequate number of coherent phonons which constitute a lossy enabling cohort.

Note that in the figure, conventional CF/LANR operation is shown above the output of ohmic controls ("normal"). Now, what was once extraordinary CF/LANR output from an active component, now appears to have been the only the 'first stage' CF/LANR.

Importantly, located at higher driving input electrical currents, the high-intensity fractionated magnetic fields treated NANOR®s (M-NANORs) demonstrate their own novel magnetic-induced optimal operating point (M-OOP) manifold curve which is located to the "right" (at higher input electrical currents) of the conventional CF/LANR OOP.

Attention is now directed to the two (2) OOP manifolds. The composite two-maximum OOP manifold of dH/dt-treated NANOR®s is complex and reflects an amplified original optimal operating point manifold AND a new OOP, apparently linked to the input electric current or power in a complex way. On close inspection, there is the development of an entirely new OOP manifold by the applied fractionated magnetic field intensity AND a modification of the previous "original" OOP manifold. The result is that there is now an amplified (phonon) OOP and a *de novo* second (magnon?) OOP manifold – these are the two OOP manifolds.

The set of several (new) dual OOP manifolds also present BOTH the synchronous and the metachronous impacts of a fractionated magnetic field intensity. Note that M-OOP for NANOR®s have different OOP characteristics, and different behavior, than conventional OOPs for NANOR®s. This suggests that these might actually reflect different methods of coupling through the lattice to the $^{4}He^{*}$. It does this by showing both the generated amplified phonon OOP and the *de novo* magnon OOP which continues during its application, and somewhat after its treatment of the CF/LANR device. These findings suggest that there are two possible paths for successful cold fusion results. Or in the

fo

Figure 7. Amplification of, and Residual Impact upon, a NANORő-type LANR Device – Instantaneous power gain for the preloaded NANORő-type LANR device under several conditions of operation. There is development of a new optimal operating point (OOP) manifold by the applied fractionated magnetic field intensity. There is also enhanced improvement of CF/LANR (which is synchronous, and here called "enhanced"), and there is improved of CF/LANR which is metachronous and longer-lasting, which is here called "improved". Conventional cold fusion and conventional ohmic thermal operation ("normal", characterized by a power gain of 1 or less) are also shown.

alternative, the magnon OOP is important because it is a 'gateway' to an entire new level of CF/LANR operation - a second stage.

3.5. dH/dt Magnetic fields can damage equipment

High intensity magnetic fields can damage equipment. There is a danger of equipment breakdown even with only 3 minutes of dH/dt treatment. This is also reflected in the electronic signals delivered.

4. Conclusion

4.1. Interpretation

It is clear that magnetically activating these preloaded nanostructured CF/LANR devices is very useful. Attention is directed to the just-discovered synchronous and metachronous impacts of a fractionated magnetic field intensity, associated with strong evidence of two (2) OOP manifolds. Astonishingly, it was discovered that there is also enhanced improvement of CF/LANR (which is synchronous), and there is improved of CF/LANR which is metachronous and longer-lasting.

The peak power gain of such treated NANOR®s (M-NANOR®s) ranged from 22 to up to ∼80 times input electrical power or more beyond the control, as determined by calorimetry. There was also an increase in energy gain, and increased incremental power gain, over ordinary cold fusion. The application of dH/dt created an increase of 4–10 times the peak power gain over conventional CF/LANR with the same system.

These treated magnetically poled NANOR®-type nanostructured LANR devices (M-NANOR®s) have functioned for more than many months after treatment, at more than one location. They are conveniently preloaded, mountable as easily activated LANR (CF) components into integrated circuits. They are activated by applied electric fields and applied fractionated magnetic fields, and are a new generation of activated CF/LANR nanocomposite ZrO_2–PdNiD electronic devices. These can be used as an effective very clean, highly efficient, energy production system, apparatus, and processes. They are integrable into microprocessor controlled integrated circuits providing a new generation of CF/LANR quantum optical devices containing preloaded nanostructured LANR materials.

Tomorrow, preloaded CF/LANR nanostructured materials and devices will be high power, high-efficiency, self-contained, auto-controlled, energy production devices. They will enable remote powering of electronic, bioelectronics, robotic, propulsion, space and avionic, and off-grid systems.

4.2. Future plans and implications

The two different OOP manifolds suggest an entirely new material science/nuclear interaction and technology. These complex responses remind one of ferro-, ferri, and antiferromagnetism, and the range of dielectric materials which are known to exist for other materials, and which are now possible here, too.

Furthermore, there may be special effects when the field is perpendicular to the direction of current through the NANOR® at the time of operation, and more work is needed to determine this with statistical certainty over clinical report.

Acknowledgements

The authors would like to thank Alex Frank, Allen Swartz, Charles Entenmann, Dennis Cravens, Dennis Letts, Brian Ahern, Jeff Driscoll, Larry Forsley, Pamela Mosier-Boss, Frank Gordon, Robert Smith, Robert Bass, David Nagel, Linda Hammond, and JET Energy and New Energy Foundation for support. NANOR® and PHUSOR® are registered

trademarks. NANOR®-technology, and PHUSOR®-technology, and other discussed IP herein, are protected by U.S. Patents D596724, D413659 and several other patents pending.

References

[1] Swartz, M., Survey of the observed excess energy and emissions in lattice assisted nuclear reactions, *J. Sci. Exploration* **23** (4) (2009) 419–436.

[2] Szpak, S., P.A. Mosier-Boss and F.E. Gordon, Further evidence of nuclear reactions in the Pd/D lattice: emission of charged particles, *Naturwissenschaften,* 94 (2007) 511–514.

[3] Bockris, J. O'M., R. Sundaresan, D. Letts and Z.S. Minevski, Triggering and structural changes in cold fusion electrodes, *Proc. ICCF4*, Maui, Hawaii, 1993.

[4] Cravens, D., Factors, Affecting success rate of at generation in CF cells, *Proc. ICCF-4,* Maui, Hawaii, USA, 1993.

[5] Bockris, J.O'M., R. Sundaresan, D. Letts and Z.S. Minevski, Triggering and structural changes in cold fusion electrodes, *ICCF4*, Maui, Hawaii, 1993, to be published.

[6] Miles, M.H., Hollins, R.A., Bush, B.F., Lagowski, J.J. and R.E. Miles, Correlation of excess power and helium production during D_2O and H_2O electrolysis, *J. Electro-analytical Chem.* **346** (1993), 99–117; Miles, M.H. and Bush, B.F., Heat and helium measurements in deuterated palladium, *Trans. Fusion Technol.* **26** (1994) 156–159.

[7] Swartz, M., Three physical regions of anomalous activity in deuterided palladium, *Infinite Energy* **14**(61) (2008) 19–31.

[8] Swartz, M., Excess power gain using high impedance and codepositional LANR devices monitored by calorimetry, at flow, and paired stirling engines, *Proc. ICCF-14*, 10–15 August 2008, Washington, D.C. ISBN: 978-0-578-06694-3, 123, (2010).

[9] Swartz, M. and G. Verner, Excess at from low electrical conductivity avy water spiral-wound Pd/D_2O/Pt and Pd/D_2O–$PdCl_2$/Pt devices, *Condensed Matter Nuclear Science*, *Proc. ICCF-10*, P. Hagelstein and S. Chubb (Eds.), World Scientific, NJ, ISBN 981-256-564-6, 29-44; 45-54 (2006).

[10] Swartz. M., The Impact of avy water (D_2O) on nickel-light water cold fusion systems, *Proc. 9th Int. Conf. on Cold Fusion (Condensed Matter Nuclear Science)*, Beijing, China, Xing Z. Li (Ed.), May 2002, pp. 335–342.

[11] Swartz, M. and G. Verner, The Phusor®-type LANR cathode is a metamaterial creating deuteron flux for excess power gain, *Proc. (ICCF-14),* 10–15 August 2008, Washington, D.C. ISBN: 978-0-578-06694-6,3, 458, (2010).

[12] Swartz, M., Photoinduced excess at from laser-irradiated electrically-polarized palladium cathodes in D_2O, *Condensed Matter Nuclear Science, Proc. ICCF-1*0, Peter L. Hagelstein and Scott Chubb (Eds.), NJ, ISBN 981-256-564-6, 213-226 (2006).

[13] Swartz, M., Can a Pd/D_2O/Pt device be made portable to demonstrate the optimal operating point? *Condensed Matter Nuclear Science, Proc. of ICCF-10*, Peter L. Hagelstein and Scott, R. Chubb (Eds.), World Scientific, NJ, ISBN 981-256-564-6, 29-44; 45-54 (2006).

[14] Swartz, M., G.Verner and A.Weinberg, Non-thermal near-IR emission from high impedance and codeposition LANR devices, *Proc. of the 14th Int. Conf. on Condensed Matter Nuclear Science and the 14th Int. Conf. on Cold Fusion (ICCF-14),* 10–15 August 2008, Washington, D.C. David J. Nagel and Michael E. Melich (Eds.), ISBN: 978-0-578-06694-3, 343, (2010).

[15] Swartz, M., Optimal operating point manifolds in active, loaded palladium linked to three distinct physical regions, *Proc. of the 14th Int. Conf. on Condensed Matter Nuclear Science and the 14th Int. Conf. on Cold Fusion (ICCF-14)*, 10–15 August 2008, Washington, D.C. David J. Nagel and Michael E. Melich (Eds.), ISBN: 978-0-578-06694-3, 639, (2010).

[16] Swartz, M., Quasi-one-dimensional model of electrochemical loading of isotopic fuel into a metal, *Fusion Technol.* **22**(2) (1992) 296–300.

[17] Swartz. M., Consistency of the biphasic nature of excess enthalpy in solid state anomalous phenomena with the quasi-1-dimensional model of isotope loading into a material, *Fusion Technol.* **31** (1997) 63–74.

[18] Swartz. M., Generality of optimal operating point behavior in low energy nuclear systems, *J. New Energy* **4**(2) (1999) 218–228.

[19] Swartz, M.R., G. Verner and J. Tolleson, Energy gain from preloaded ZrO_2–PdNi–D nanostructured CF/LANR quantum electronic components, *Proc. of the 17th Int. Conf. on Condensed Matter Nuclear Science and the 17th Int. Conf. on Cold Fusion (ICCF-17; pending)* (2012).

[20] Swartz. M. and P.L.Hagelstein, Demonstration of energy gain from a preloaded ZrO_2–PdD nanostructured CF/LANR quantum electronic device at MIT, *Proc. ICCF17* (2012).

[21] Swartz, M., LANR nanostructures and metamaterials driven at their optimal operating point, *Third Volume of the LANR/LENR Sourcebook*, October 21, 2011.
[22] Swartz. M., P. Mosier-Boss, P.L. Hagelstein, G, Verner, J, Tolleson, L. Wright and R. Goldbaum, Imaging of an active LANR quantum electronic component using CR-39 confirmation of LANR nuclear activity and emission of penetrating ionizing radiation temporally, spatially, and by imaging, *Proc. of the 18th Int. Conf. on Condensed Matter Nuclear Science and the 18th Int. Conf. on Cold Fusion (ICCF-18)*, Minnesota, 2013.
[23] Swartz. M., Incremental high energy emission from a ZrO_2–Pd-D nanostructured CF/LANR quantum electronic component, *Proc. of the 18th Int. Conf. on Condensed Matter Nuclear Science and the 18th Int. Conf. on Cold Fusion (ICCF-18)*, Minnesota, 2013.
[24] Swartz, M.R. Impact of an applied magnetic field on the electrical impedance of a LANR device, *Proc. of JCMNS*, Vol. 4, March 2010, *New Energy Technology Symposium* held at the 239th American Chemical Society National Meeting and Exposition in San Francisco (2011).
[25] Santos, D.L.R., P. Venezuela, R.B. Muniz and A.T. Costa, Spin pumping and interlayer exchange coupling through palladium, *Phys. Rev. B* **88** (2013) 054423.
[26] Shimizu, Sunao, Kei S. Takahashi, Takafumi Hatano, Masashi Kawasaki, Yoshinori Tokura, and Yoshihiro Iwasa, Electrically tunable anomalous hall effect in Pt thin films, *Phys. Rev. Lett*. **111** (2013) 216803.
[27] Sun, Y., J.D. Burton and E.Y. Tsymbal, Electrically driven magnetism on a Pd thin film, *Phys. Rev.* B **81** (2010) 064413.
[28] Takanol, N., T. Kai2, K.Shiiki2 and F.Terasakil, Effect of copious vacancies on magnetism of Pd, *Solid State Commun.* **97**(2) (1996) 153–156.
[29] Swartz, M, Magnetic imaging of a NANOR using a horizontal translated hall effect sensor, (2014) in preparation.